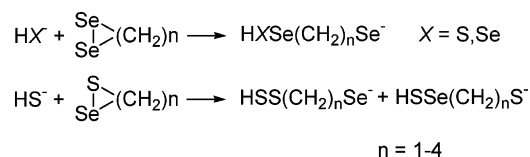


## Effect of Ring Strain on Nucleophilic Substitution at Selenium: A Computational Study of Cyclic Diselenides and Selenenyl Sulfides

Steven M. Bachrach,\* Claire J. Walker, Fiona Lee, and Sarah Royce  
 Department of Chemistry, Trinity University, 1 Trinity Place, San Antonio, Texas 78212

sbachrach@trinity.edu

Received March 20, 2007



Nucleophilic substitution reactions of small rings incorporating selenium are examined using computational methods. The potential energy surfaces of  $\text{HS}^-$  and  $\text{HSe}^-$  with 1,2-diselenirane, 1,2-diselenetane, 1,2-diselenolane, and 1,2-diselenane were computed at B3LYP/6-31+G(d) and MP2/6-31+G(d). The reactions of three-, four-, five-, and six-membered rings incorporating the S–Se bond with  $\text{HS}^-$  were computed at B3LYP/6-31+G(d). The strained three- and four-membered diselenides and selenenyl sulfide rings undergo  $\text{S}_{\text{N}}2$  reactions, while the five- and six-membered rings react via the addition–elimination pathway, a path that invokes a hypercoordinate selenium intermediate. The strain in the small rings precludes the addition of a further ligand to either heteroatom. Substitution at selenium is both kinetically and thermodynamically favored over attack at sulfur.

### Introduction

Nucleophilic substitution remains one of the pillars of mechanistic principle developed within the realm of physical organic chemistry. The  $\text{S}_{\text{N}}1$  and  $\text{S}_{\text{N}}2$  mechanisms are well-understood for reactions at carbon.<sup>1</sup> Our recent work has been focused on the nature of nucleophilic substitution at heteroatoms, specifically at oxygen,<sup>2</sup> phosphorus,<sup>3</sup> sulfur, and selenium, using computational means. For nucleophilic substitution at sulfur, the Hartree–Fock method predicts a standard  $\text{S}_{\text{N}}2$  mechanism for the gas phase, with a single transition state on the potential energy surface (PES).<sup>4</sup> This turns out to be an artifact of omitting electron correlation. With a variety of methods that include electron correlation to some extent—MP2, DFT, and CI—what was the HF transition state is actually a local energy minimum.<sup>5,6</sup> The gas-phase mechanism is addition–elimination (A–E): the nucleophile adds to sulfur, forming a hypercoordinate anionic intermediate, and in a second distinct chemical step, the leaving group exits. The addition–elimination mechanism operates in a variety of sulfur environments—acyclic monosulfides,<sup>7</sup> dis-

ulfides,<sup>5,8</sup> and trisulfides.<sup>9</sup> The extreme case is the reaction  $\text{SCl}_2 + \text{Cl}^-$  where the only critical point (besides reactant and products) on the PES is the hypercoordinate species  $\text{SCl}_3^-$ .<sup>10</sup> The  $\text{S}_{\text{N}}2$  mechanism operates when the sulfur is placed into a very strained environment, such as dithirane and 1,2-dithietane, but the larger and less strained rings, 1,2-dithiolane and 1,2-dithiane, undergo nucleophilic substitution via the A–E path.<sup>11,12</sup>

Our initial studies of nucleophilic substitution at selenium found results very similar to those for substitution at sulfur. The HF method again fails to locate the hypercoordinate intermediate. Both MP2 and B3LYP predict topologically identical PESs that indicate an addition–elimination mechanism for substitution in acyclic diselenides.<sup>13</sup> The reaction  $\text{SeCl}_2 + \text{Cl}^-$  has a single critical point corresponding to the hypercoordinate intermediate  $\text{SeCl}_3^-$ .<sup>14</sup> One important difference is that

(1) (a) Lowry, T. H.; Richardson, K. S. *Mechanism and Theory in Organic Chemistry*, 3rd ed.; Harper and Row: New York, 1987. (b) Carroll, F. A. *Perspectives on Structure and Mechanism in Organic Chemistry*; Brooks/Cole Publishing: Pacific Grove, CA, 1997.

(2) Bachrach, S. M. *J. Org. Chem.* **1990**, *55*, 1016–1019.

(3) Bachrach, S. M.; Mulhearn, D. C. *J. Phys. Chem.* **1993**, *97*, 12229–12231.

(4) Aida, M.; Nagata, C. *Chem. Phys. Lett.* **1984**, *112*, 129–132.

(5) Bachrach, S. M.; Mulhearn, D. C. *J. Phys. Chem.* **1996**, *100*, 3535–3540.

(6) Bachrach, S. M.; Hayes, J. M.; Dao, T.; Mynar, J. L. *Theor. Chem. Acc.* **2002**, *107*, 266–271.

(7) Bachrach, S. M.; Gailbreath, B. D. *J. Org. Chem.* **2001**, *66*, 2005–2010.

(8) Bachrach, S. M.; Chamberlin, A. C. *J. Org. Chem.* **2003**, *68*, 4743–4737.

(9) Mulhearn, D. C.; Bachrach, S. M. *J. Am. Chem. Soc.* **1996**, *118*, 9415–9421.

(10) Gailbreath, B. D.; Pommerening, C. A.; Bachrach, S. M.; Sunderlin, L. S. *J. Phys. Chem. A* **2000**, *104*, 2958–2961.

(11) Bachrach, S. M.; Woody, J. T.; Mulhearn, D. C. *J. Org. Chem.* **2002**, *67*, 8983–8990.

(12) Fernandes, P. A.; Ramos, M. J. *Chem.—Eur. J.* **2004**, *10*, 257–266.

(13) Bachrach, S. M.; Demoin, D. W.; Luk, M.; Miller, J. V., Jr. *J. Phys. Chem. A* **2004**, *108*, 4040–4046.

(14) Lobring, K. C.; Hao, C.; Forbes, J. K.; Ivanov, M. R. J.; Bachrach, S. M.; Sunderlin, L. S. *J. Phys. Chem. A* **2003**, *107*, 11153–11160.

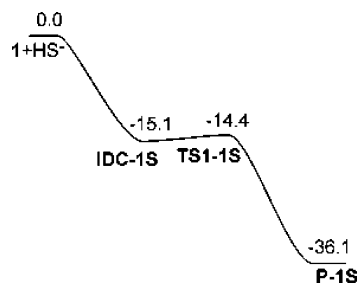
substitution at selenium is thermodynamically and kinetically more favorable than at sulfur.

Very little experimental work has been reported on the nature of nucleophilic substitution at either the S–Se or Se–Se bond. Kice and Slebocka-Tilk examined the reaction  $RSSeSR + RSH$  with  $R = n\text{-Bu}$ ,  $i\text{-Pr}$ , or  $t\text{-Bu}$ .<sup>15</sup> They found that the nucleophile is thiolate, not thiol, and that attack at selenium is generally faster than attack at sulfur. Rabenstein and co-workers found similar results—attack at selenium is faster than at sulfur for the reactions D-penicillamine (PSH) with bis(D-penicillamine)-selenide (PSSeSP) and  $t\text{-BuS}^- + t\text{-BuSSeSBu-}t$ .<sup>16</sup> Recent studies by Sarma and Mugesh suggest that proximal interactions with nitrogen and oxygen can be used to enhance nucleophilic attack at either sulfur or selenium in selenenyl sulfides, though attack at the selenium is generally preferred.<sup>17</sup> For the case of substitution reactions of diselenides, Rabenstein examined the reaction  $R^*\text{SeH} + R\text{SeSeR}$  where  $R$  is  $\text{H}_3\text{NCH}_2\text{CH}_3$  and  $R^*$  is a selectively deuterated analogue.<sup>18</sup> The nucleophile is selenolate, not the selenol, similar to the thiol–disulfide exchange and reactions of selenenyl sulfides. Of greater interest here is that the exchange reaction with diselenide is  $10^7$  times faster than the reaction of identically substituted disulfide. Rabenstein argued that selenium is more polarizable than sulfur, making it both a better nucleophile and leaving group. Nucleophilic cleavage of the Se–Se bond has been exploited for synthetic purposes.<sup>19</sup>

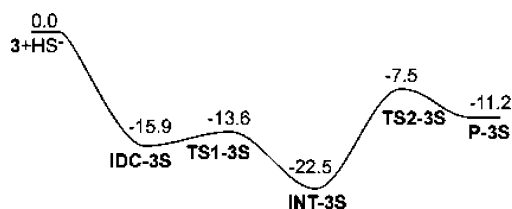
The purpose of this study is twofold. First, we examine gas-phase nucleophilic substitution at a selenium atom of cyclic diselenides. This extends our previous work with acyclic diselenides<sup>13</sup> and offers the comparison with the cyclic disulfides.<sup>11</sup> We utilize  $\text{HS}^-$  and  $\text{HSe}^-$  as the nucleophile for comparison with our previous studies and also to compare the relative nucleophilicity of sulfur versus that of selenium. Second, we examine nucleophilic substitution of cyclic selenenyl sulfides, comparing the selectivity of substitution toward selenium versus sulfur. Thiolate is used as the nucleophile as a model of the cellular nucleophile glutathione.

We hope these latter model systems will provide some insight as to the role of selenium in selenoproteins. Selenium-containing proteins comprise an unusual yet important class of biologically necessary compounds.<sup>20</sup> Examples of selenoproteins include glutathione peroxidase,<sup>21</sup> thioredoxin reductase,<sup>22</sup> and iodothyronine deiodinase.<sup>23</sup> These proteins incorporate a selenocysteine residue that invariably makes a S–Se bridge with a cysteine

SCHEME 1. PES for Reaction 1S



SCHEME 2. PES for Reaction 3S



residue. This S–Se linkage is implicated in the activity of many selenoproteins, being cleaved through redox reactions or nucleophilic attack at either heteroatom.<sup>24</sup> It should be realized that the computations we report here are for the gas phase and so their direct applicability to solution-phase enzymatic systems may be limited. A follow-up study incorporating solvent is underway and will better address this issue.

## Computational Methods

In order to assess the selectivity for attack at sulfur versus selenium, we first examined nucleophilic attack by either thiolate ( $\text{HS}^-$ ) or hydrogen selenide ( $\text{HSe}^-$ ) at selenium in the three-, four-, five-, and six-membered cyclic diselenides (1–4). These reactions are labeled as Reaction 1x–4x, where  $x$  is S or Se to indicate the nucleophile. As is typical for a gas-phase nucleophilic substitution reaction,<sup>25</sup> an ion–dipole complex is first formed along the reaction path; these are labeled as **IDC-Nx**, where  $N$  designates the reaction number and  $x$  again designates the nucleophile. Next, a transition state is located and designated as **TS1-Nx**. If the reaction mechanism is  $\text{S}_{\text{N}}2$ , the next critical point located is the product, **P-Nx**. If the mechanism is addition–elimination, an intermediate, **INT-Nx**, occurs next, followed by an exit transition state, **TS2-Nx**. To complete the reaction, we located the product (**P-Nx**) conformation that directly results from the exit transition state. In some cases, we located other product conformations and the structure that results from intramolecular proton transfer (**PTP-Nx**). Sketches of the potential energy surface for both the  $\text{S}_{\text{N}}2$  and addition–elimination pathways with all critical points identified are shown in Schemes 1 and 2.

Nucleophilic attack on cyclic selenenyl sulfides was examined in an analogous fashion. Thiolate served as the nucleophile. Reactions 5–8 denote attack at the three-, four-, five-, and six-membered rings (5–8), respectively. In labeling the critical points along these reactions, we use the same scheme as described above,

(15) Kice, J. L.; Slebocka-Tilk, H. *J. Am. Chem. Soc.* **1982**, *104*, 7123–7130.

(16) Rabenstein, D. L.; Scott, T. M.; Guo, W. *J. Org. Chem.* **1991**, *56*, 4176–4181.

(17) (a) Sarma, B. K.; Mugesh, G. *J. Am. Chem. Soc.* **2005**, *127*, 11477–11485. (b) Sarma, B. K.; Mugesh, G. *Inorg. Chem.* **2006**, *45*, 5307–5314.

(18) Pleasants, J. C.; Guo, W.; Rabenstein, D. L. *J. Am. Chem. Soc.* **1989**, *111*, 6553–6558.

(19) (a) Vasil'ev, A.; Engman, L. *J. Org. Chem.* **2000**, *65*, 2151–2162.

(b) Henriksen, L.; Stühr-Hansen, N. *J. Chem. Soc., Perkin Trans. 1* **1999**, 1915–1916. (c) Engman, L.; Gupta, V. *J. Org. Chem.* **1997**, *62*, 157–173.

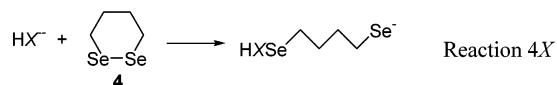
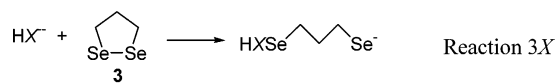
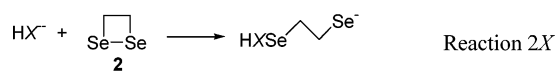
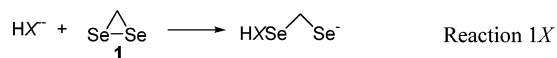
(d) Engman, L.; Stern, D. *J. Org. Chem.* **1994**, *59*, 5179–5183.

(20) (a) Hadaszadeh, B. M.; Beggs, A. H. *Physiology* **2006**, *21*, 307–315. (b) Gromer, S.; Eubel, J. K.; Lee, B. L.; Jacob, J. *Cell. Mol. Life Sci.* **2005**, *62*, 2414–2437. (c) Chen, J.; Berry, M. J. *J. Neurochem.* **2003**, *86*, 1–12. (d) Behne, D.; Kyriakopoulos, A. *Annu. Rev. Nutrition* **2001**, *21*, 453–473. (e) Stadtman, T. C. *J. Biol. Chem.* **1991**, *266*, 16257–16260.

(21) (a) Flohe, L.; Günzler, W. A.; Schock, H. H. *FEBS Lett.* **1973**, *32*, 132–134. (b) Rotruck, J. T.; Pope, A. L.; Ganther, H. E.; Swanson, A. B.; Hafeman, D. G.; Hoekstra, W. G. *Science* **1973**, *179*, 588–590. (c) Epp, O.; Ladenstein, R.; Wendel, A. *Eur. J. Biochem.* **1983**, *51*–69. (d) Ren, B.; Huang, W.; Åkesson, B.; Ladenstein, R. *J. Mol. Biol.* **1997**, *268*, 869–885.

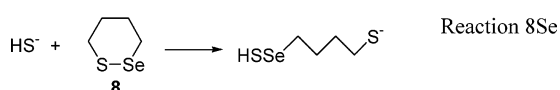
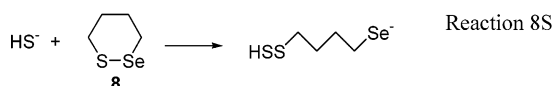
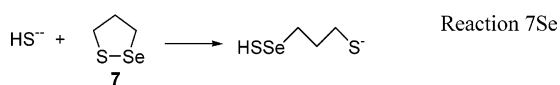
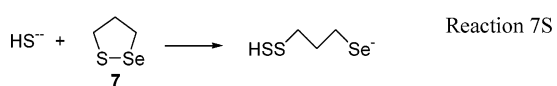
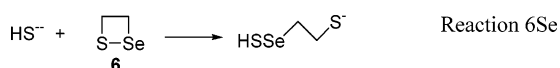
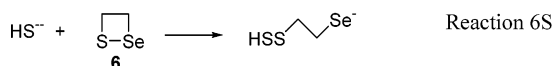
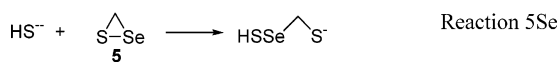
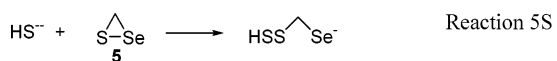
(22) (a) Tamura, T.; Stadtman, T. C. *Proc. Natl. Acad. Sci. U.S.A.* **1996**, *93*, 1006–1011. (b) Lee, S.-R.; Kim, J.-R.; Kwon, K.-S.; Yoon, H. W.; Levine, R. L.; Ginsburg, A.; Rhee, S. G. *J. Biol. Chem.* **1999**, *274*, 4722–4734. (c) Mustacich, D.; Powis, G. *Biochem. J.* **2000**, *346*, 1–8. (d) Sandalova, T.; Zhong, L.; Lindqvist, Y.; Holmgren, A.; Schneider, G. *Proc. Natl. Acad. Sci. U.S.A.* **2001**, *98*, 9533–9538.

(23) (a) Behne, D.; Kyriakopoulos, A.; Meinhold, H.; Köhrle, J. *Biochem. Biophys. Res. Commun.* **1990**, *173*, 1143–1149. (b) Berry, M. J.; Banu, L.; Larsen, P. R. *Nature* **1991**, *349*, 438–440. (c) St. Germain, D. L. *Trends Endocrinol. Metab.* **1994**, *5*, 36–42.



X = S, Se

except now the trailing x designates whether the nucleophile has attacked the sulfur (S) or selenium (Se) atom in the ring.



As discussed in the Introduction, Hartree–Fock theory incorrectly predicts the topology of the potential energy surface for nucleophilic substitution at sulfur and selenium.<sup>5,13</sup> However, once electron correlation is included, no matter the manner, similar topologies are found. There are noticeable differences in relative energies of the critical points as determined by different computational methods. We would like to make use of DFT methods for the study of Reactions 5–8 to minimize computational costs. In order to gauge the relative errors in the energies of the critical points, we have

(24) (a) Johansson, L.; Gafvelin, G.; Arner, E. S. *J. Biochim. Biophys. Acta* **2005**, *1726*, 1–13. (b) Zhong, L. W.; Arner, E. S. J.; Holmgren, A. *Proc. Natl. Acad. Sci. U.S.A.* **2000**, *97*, 5854–5859. (c) Arner, E. S. J.; Holmgren, A. *Eur. J. Biochem.* **2000**, *267*, 6102–6109. (d) Mughesh, G.; du Mont, W. W.; Wismach, C.; Jones, P. G. *ChemBioChem* **2002**, *3*, 440–447. (e) Ma, S.; Hill, K. E.; Burk, R. F.; Caprioli, R. M. *Biochemistry* **2003**, *42*, 9703–9711.

(25) (a) Brauman, J. I.; Olmstead, W. N.; Lieder, C. A. *J. Am. Chem. Soc.* **1974**, *96*, 4030–4031. (b) Olmstead, W. N.; Brauman, J. I. *J. Am. Chem. Soc.* **1977**, *99*, 4219–4278. (c) Pellerite, M. J.; Brauman, J. I. *J. Am. Chem. Soc.* **1980**, *102*, 5993–5999. (d) Wilbur, J. L.; Brauman, J. I. *J. Am. Chem. Soc.* **1991**, *113*, 9699–9701.

examined Reactions 1–4 at MP2/6-31+G(d) and B3LYP/6-31+G(d).<sup>26</sup> This complements our previous study of nucleophilic substitution of cyclic disulfides.<sup>11</sup> (We also examined the reaction  $\text{HS}^- + \text{MeSSeMe}$  with a number of different basis sets and methods.) Geometries of all critical points were completely optimized with these two methods. Analytical frequencies were computed, and the resulting zero-point vibrational energies were used without further correction. The critical points for Reaction 5–8 were obtained at B3LYP/6-31+G(d). All computations were performed using Gaussian 03.<sup>27</sup>

## Results

**Substitution of Cyclic Diselenides.** All critical points along Reactions 1S–4S and 1Se–4Se were optimized at both B3LYP and MP2. The geometries obtained with these two methods are generally quite similar; a few exceptions will be noted below. Additionally, the overall structure of the critical points are analogous whether the nucleophile is  $\text{HS}^-$  or  $\text{HSe}^-$ . So for simplicity, we display in Figures 1 and 2 the structures of the critical points for Reactions 2 and 3 with  $\text{HS}^-$ , respectively. These figures demonstrate the various types of critical points found in all of the reactions we present here. (Drawings of the critical points for Reactions 1 and 4 with  $\text{HSe}^-$  are presented in Figure S1 and S2, and the coordinates of all critical point structures are given in the Supporting Information.)

As noted many times for gas-phase reactions involving an anion and a neutral substrate,<sup>25</sup> an ion–dipole complex (IDC) is the first critical point along all of these reactions. These IDCs are formed by the attraction of either the negatively charged S or Se for the partially positively charged hydrogen atoms of the rings. There are many potential configurations of ion–dipole structures, with the anionic heteroatom associated with only one hydrogen atom or bridging across multiple hydrogen atoms. We have not attempted an exhaustive search of the IDC space, but rather located a viable representative of the IDC collection for each reaction. For this reason, the following transition state may be lower in energy than the IDC we have located.

The next critical point along each reaction pathway is a transition structure where the nucleophile begins to swing toward a selenium atom of the ring while also weakening the interaction with the hydrogen atom(s). These transition states (**TS1**) all involve long separations (greater than 4 Å) between the incoming heteroatom and the ring selenium atom. This is consistent behavior with what we observed in the nucleophilic substitution reactions of cyclic disulfides.<sup>11</sup>

(26) (a) Becke, A. D. *J. Chem. Phys.* **1993**, *98*, 5648–5650. (b) Lee, C.; Yang, W.; Parr, R. G. *Phys. Rev. B* **1988**, *37*, 785–789. (c) Vosko, S. H.; Wilk, L.; Nusair, M. *Can. J. Phys.* **1980**, *58*, 1200–1211. (d) Stephens, P. J.; Devlin, F. J.; Chabalowski, C. F.; Frisch, M. J. *J. Phys. Chem.* **1994**, *98*, 11623–11627.

(27) Frisch, M. J.; Trucks, G. W.; Schlegel, H. B.; Scuseria, G. E.; Robb, M. A.; Cheeseman, J. R.; Montgomery, J. A., Jr.; Vreven, T.; Kudin, K. N.; Burant, J. C.; Millam, J. M.; Iyengar, S. S.; Tomasi, J.; Barone, V.; Mennucci, B.; Cossi, M.; Scalmani, G.; Rega, N.; Petersson, G. A.; Nakatsuji, H.; Hada, M.; Ehara, M.; Toyota, K.; Fukuda, R.; Hasegawa, J.; Ishida, M.; Nakajima, T.; Honda, Y.; Kitao, O.; Nakai, H.; Klene, M.; Li, X.; Knox, J. E.; Hratchian, H. P.; Cross, J. B.; Bakken, V.; Adamo, C.; Jaramillo, J.; Gomperts, R.; Stratmann, R. E.; Yazyev, O.; Austin, A. J.; Cammi, R.; Pomelli, C.; Ochterski, J. W.; Ayala, P. Y.; Morokuma, K.; Voth, G. A.; Salvador, P.; Dannenberg, J. J.; Zakrzewski, V. G.; Dapprich, S.; Daniels, A. D.; Strain, M. C.; Farkas, O.; Malick, D. K.; Rabuck, A. D.; Raghavachari, K.; Foresman, J. B.; Ortiz, J. V.; Cui, Q.; Baboul, A. G.; Clifford, S.; Cioslowski, J.; Stefanov, B. B.; Liu, G.; Liashenko, A.; Piskorz, P.; Komaromi, I.; Martin, R. L.; Fox, D. J.; Keith, T.; Al-Laham, M. A.; Peng, C. Y.; Nanayakkara, A.; Challacombe, M.; Gill, P. M. W.; Johnson, B.; Chen, W.; Wong, M. W.; Gonzalez, C.; Pople, J. A. *Gaussian 03*, revision D.01; Gaussian, Inc.: Wallingford, CT, 2004.

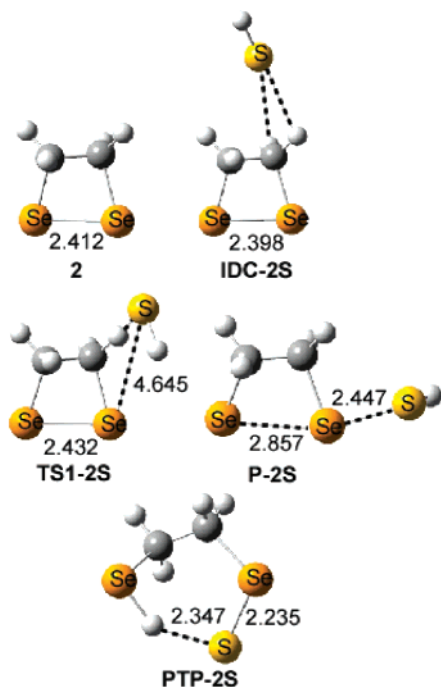


**FIGURE 1.** B3LYP/6-31+G(d) optimized geometries of the critical points for Reaction 2S. All distances are in angstroms.

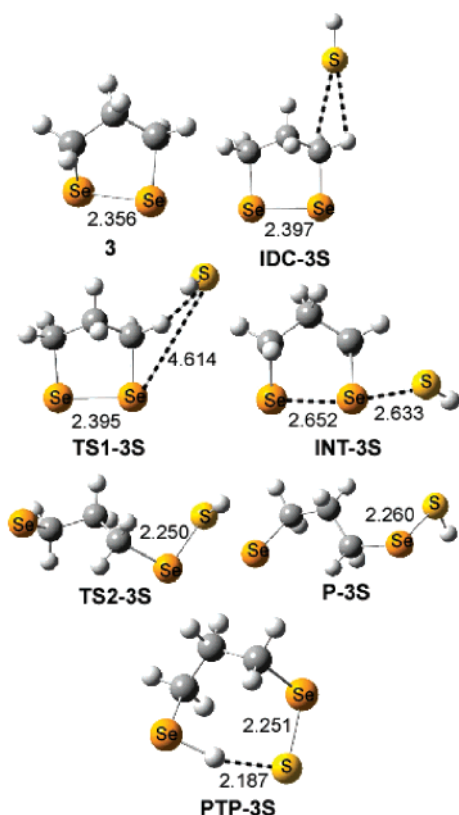


**FIGURE 2.** B3LYP/6-31+G(d) optimized geometries of the critical points for Reaction 3S. All distances are in angstroms.

The nature of the pathway for Reactions 1 and 2 diverges from the others after **TS1**. For these four reactions, as the nucleophile continues to move toward a selenium atom, the Se–Se bond ruptures, so that the next critical point is the substitution

**TABLE 1.** Geometric Parameters of **P-2**, **INT-3**, and **INT-4**<sup>a</sup>

	<i>r</i> - (Se–Se)	<i>r</i> - (Se–X)	<i>a</i> - (Se–Se–X)		<i>r</i> - (Se–Se)	<i>r</i> - (Se–X)	<i>a</i> - (Se–Se–X)
<b>P-2S</b>	2.857	2.447	163.2	<b>P-2Se</b>	2.850	2.559	161.8
	2.871	2.366	161.9		2.786	2.546	160.9
<b>INT-3S</b>	2.652	2.633	171.7	<b>INT-3Se</b>	2.665	2.710	169.7
	2.672	2.507	170.2		2.632	2.669	168.0
<b>INT-4S</b>	2.609	2.707	176.0	<b>INT-4Se</b>	2.623	2.773	174.4
chair	2.629	2.563	172.9	chair	2.591	2.724	172.1
<b>INT-4S</b>	2.691	2.631	174.2	<b>INT-4Se</b>	2.698	2.710	174.2
boat	2.701	2.513	173.4	boat	2.650	2.679	172.3

<sup>a</sup> All distances are in angstroms, and angles are in degrees. X represents S or Se of the nucleophile. B3LYP/6-31+G(d) values are in normal font, and MP2/6-31+G(d) values are in italics.

product **P-1** or **P-2**. Here, the bond between the nucleophile heteroatom and selenium is fully formed, and what was the Se–Se bond of the three- or four-membered ring is broken. (We defer further discussion of **P-2** to where we present the intermediates of Reactions 5–8, but note that their geometrical parameters are listed in Table 1.) Conformational rotation can bring the ends of the chain in proximity, at which point the proton transfers to yield **PTP-1** or **PTP-2**.

For the other four substitution reactions of cyclic diselenides, forward progress from **TS1** leads to an intermediate (**INT**) possessing a hypercoordinate selenium atom. All of these structures possess only real frequencies, confirming that they are local minima. Critical parameters of these intermediates (the Se–Se distance within the ring, the Se–X distance, and the Se–Se–X angles, where X is either S or Se of the nucleophile) are listed in Table 1. For comparison purposes, typical Se–Se distances in the intermediates of a substitution reaction involving acyclic diselenides are 2.67–2.70 (B3LYP) or 2.64–2.66 Å (MP2). The B3LYP S–Se and Se–Se distances in the intermediate for the reaction  $\text{HS}^- + \text{CH}_3\text{SeSeCH}_3$  are 2.716 and 2.580 Å, respectively. While the Se–Se distance is little changed at MP2 (2.608 Å), MP2 predicts that the S–Se distance is much shorter, 2.567 Å. The intermediates for Reactions 3 and 4 have distances that match up well with the acyclic analogues. MP2 and DFT values are in good agreement, except again where the Se–X MP2 distance is about 0.1 Å shorter than that predicted by B3LYP.

The structures of the intermediates follow a simple trend. As the ring gets larger, the intermediate geometry approaches that of the acyclic intermediates. The smaller the ring, the more the ring Se–Se bond is lengthened, the shorter the Se–nucleophile distance, the more nonlinear the Se–Se–X angle.

From the intermediates, these reactions pass over an exit transition state (**TS2**). The atomic motion associated with the reaction coordinate for these transition states is predominantly rotation about a single bond, relieving the eclipsing interactions. So, for example, **TS2-3S** looks like a transition state simply for rotation about one of the C–C bonds, with all groups eclipsed about this bond. Rotation about the C–C bond, moving the terminal selenium in one direction, leads to the product of the substitution reaction **P-3**. Rotation in the opposite direction moves toward a *gauche*-like structure, but as the two selenium atoms approach, they form a partial bond, yielding the intermediate **INT-3S**. This same analysis applies to all four second transition states (**TS2**)—they connect intermediates (**INT**) with the substitution products (**P**).

We have optimized the conformation of the product that is the direct result of **TS2**; other conformations are possible, and some may be lower in energy. In all cases, if the two ends of

**TABLE 2.** Energies (kcal mol<sup>-1</sup>) Relative to Isolated Reactants for Reactions 1–4<sup>a</sup>

Reaction	IDC	TS1	INT	TS2	P	PTP
1Se	-13.35 <i>-15.50</i>	-15.12 <i>-16.77</i>			-38.37 <i>-36.58</i>	-38.85
2Se	-17.12 <i>-19.16</i>	-14.33 <i>-16.99</i>			-34.46 <i>-35.31</i>	-37.19
3Se	-14.88 <i>-17.46</i>	-14.20 <i>-16.56</i>	-23.98 <i>-25.17</i>	-6.46 <i>-7.04</i>	-11.17 <i>-12.50</i>	-25.04
4Se (chair)	-12.85 <i>-16.24</i>	-13.74 <i>-16.77</i>	-22.79 <i>-24.37</i>	-4.64 <i>-5.91</i>	-6.13 <i>-7.42</i>	-17.81
4Se (boat) <sup>b</sup>	-8.80 <i>-12.71</i>	-9.02 <i>-10.69</i>	-19.60 <i>-21.21</i>	-2.07 <i>-3.66</i>		
1S	-13.10 <i>-15.13</i>	-13.15 <i>-14.40</i>			-35.24 <i>-36.09</i>	-29.14
2S	-16.14 <i>-18.19</i>	-12.15 <i>-15.13</i>			-30.95 <i>-34.14</i>	-27.25
3S	-12.95 <i>-15.91</i>	-11.03 <i>-13.56</i>	-20.31 <i>-22.54</i>	-2.47 <i>-7.53</i>	-6.24 <i>-11.22</i>	-13.76
4S (chair)	-10.23 <i>-13.45</i>	-9.90 <i>-12.60</i>	-18.50 <i>-20.79</i>	0.78 <i>-4.16</i>	-0.82 <i>-5.82</i>	-6.61
4S (boat) <sup>b</sup>	-5.34 <i>-8.99</i>	-4.35 <i>-7.54</i>	-14.77 <i>-17.71</i>	2.94 <i>-2.21</i>		

<sup>a</sup> B3LYP/6-31+G(d) energies in normal font, and MP2/6-31+G(d) energies are in italics. Energies include ZPE evaluated at the same level.

<sup>b</sup> Energies relative to the chair conformation of **4**. **4**(boat) are 5.83 (B3LYP and MP2) kcal mol<sup>-1</sup> higher in energy than **4**(chair).

the products approach, the proton transfers from what was the nucleophile to the leaving anionic selenium, producing the more stable terminal Se-X anion, which we label as **PTP** for proton-transfer product. We have not searched for a transition state for this proton transfer.

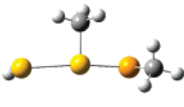
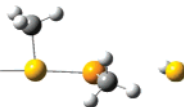
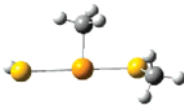
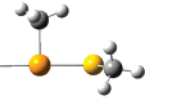
The energies of the critical points for the eight reactions of cyclic diselenides relative to isolated reactants are listed in Table 2. Energies are reported for both B3LYP and MP2 computations. Reactions 1 and 2, with either nucleophile, take place on a potential energy surface with two minima, corresponding to the IDC and product. This surface is sketched in Scheme 1 for Reaction 1S. This double-well topology is predicted by both B3LYP and MP2. The latter method predicts a more stable IDC and TS than does B3LYP, but these differences are less than 2 kcal mol<sup>-1</sup>. Schaefer noted that B3LYP activation barriers are typically underestimated by about 2 kcal mol<sup>-1</sup> for S<sub>N</sub>2 reactions.<sup>28</sup> Our computations actually indicate the opposite—the B3LYP barriers for the reverse reaction are up to a couple of kcal mol<sup>-1</sup> higher than that predicted by MP2. However, it is the shape of the potential energy surface that is the most critical point of our studies, and both methods agree that Reactions 1 and 2 have just a single transition state. The reaction with HSe<sup>-</sup> has a slightly lower barrier than the reaction with HS<sup>-</sup>, and it is also more exothermic.

Reactions 3 and 4 with HS<sup>-</sup> or HSe<sup>-</sup> follow a PES with three minima: the IDC, intermediate, and product. The PES for Reaction 3S, representative of all four reactions, is drawn in Scheme 2. For Reaction 4, we have identified the critical points for the reaction through both the chair and boat conformations of **4**; the former is more favorable, as are all of the critical points for reaction involving the chair conformer.

Both MP2 and B3LYP predict the same three-well topology for Reactions 3 and 4. MP2 predicts all of the critical points to be more stable, relative to their appropriate isolated reactants, than does B3LYP. These differences can be upward of 5 kcal mol<sup>-1</sup>. A more critical evaluation of the energies is the depth of the well associated with the intermediate, the structure that most critically defines the reaction mechanism. The well depth is evaluated as the entrance barrier  $E(\text{TS1}) - E(\text{INT})$  and exit barrier  $E(\text{TS2}) - E(\text{INT})$ . The exit barrier is higher than the entrance barrier by about 8–10 kcal mol<sup>-1</sup>. The maximum difference in the MP2 and B3LYP barrier heights is less than 2.8 kcal mol<sup>-1</sup>, and both computational methods agree as to which barrier is higher. Given the recent studies showing some serious systemic problems of B3LYP, especially notable with increasing size of the molecule under study,<sup>29</sup> B3LYP mimics well the results obtained with MP2 for these nucleophilic substitution reactions. Most important for this study, B3LYP reproduces the topology of the PES while underestimating the stability of critical points by only a few kcal mol<sup>-1</sup>.

**Substitution of Cyclic Selenenyl Sulfides.** Given that B3LYP adequately reproduces the MP2 PES, especially its topology, for Reactions 1–4 and for the reactions of thiolate with cyclic disulfides,<sup>11</sup> we were inclined to examine Reactions 5–8 at B3LYP/6-31G(d) only. In order to support this decision, we computed the relative energies of the intermediates formed by the reaction of HS<sup>-</sup> at either sulfur or selenium of MeSSeMe using a number of different methods and basis sets. This tests the ability of B3LYP to differentiate attack at sulfur from selenium, a critical point of our study, and also augments our previous work. The results are shown in Table 3. There are actually two intermediates for attack at each heteroatom, differing by the orientation of the methyl group on the central heteroatom. The relative ordering of the four intermediates is essentially identical with all methods (MP2 and two different DFT procedures, including PBE1PBE<sup>30</sup> which is thought to deal well with weak interactions<sup>31</sup> and basis sets). Most important is that all methods, including B3LYP/6-31+G(d), indicate that the intermediate from attack at selenium is more stable than that from attack at sulfur. Also noteworthy is that our choice of the small 6-31+G(d) basis set provides energies quite similar

**TABLE 3.** Relative Energies (kcal mol<sup>-1</sup>) of the Intermediates for the Reaction HS<sup>-</sup> + MeSSeMe

	HS-S(CH <sub>3</sub> )-SeCH <sub>3</sub>		HS-Se(CH <sub>3</sub> )-SCH <sub>3</sub>	
				
B3LYP/6-31+G(d) <sup>a</sup>	5.94	6.24	0.03	0.0
B3LYP/6-311+G(2d,p) <sup>a</sup>	6.68	6.76	0.05	0.0
PBE1PBE/6-311+G(2d,p) <sup>a</sup>	7.22	7.11	0.04	0.0
MP2/6-31+G(d) <sup>b</sup>	5.69	6.26	0.05	0.0
MP2/6-311+G(2d,p) <sup>b</sup>	7.58	7.59	0.0	0.06

<sup>a</sup> Corrected with ZPE at B3LYP/6-31+g(d). <sup>b</sup> Corrected with ZPE at MP2/6-31+G(d).

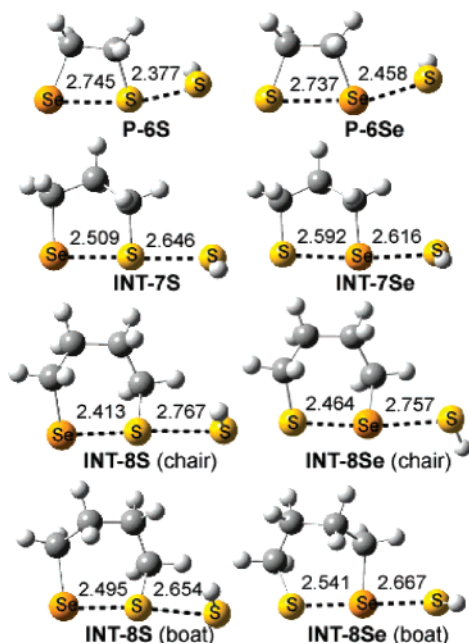


FIGURE 3. B3LYP/6-31+G(d) optimized structures of **P-6** and intermediates of Reactions 7 and 8. All distance are in angstroms.

to that with the larger basis set, and if anything it *underestimates* the preference for attack at selenium.

The potential energy surfaces of Reactions 5–8 were therefore computed at B3LYP/6-31G(d). These surfaces are very similar to their diselenide (vide supra) and disulfide<sup>11</sup> analogues. The reactants first come together to form ion dipole complexes characterized by a weak interaction between the thiolate sulfur and hydrogen atom(s) of the ring compound. We assume that a single IDC is the start for both attack at S and Se. Next, the thiolate swings toward either the ring sulfur or selenium atom, passing through the entrance transition state. For both of the reactions of the three-membered ring **5** and the four-membered ring **6**, forward progress from the entrance transition states leads directly to a ring-opened product. For Reactions 7 and 8, an intermediate results from the attack at either S or Se. A second transition state then leads to cleaving of the S–Se bond of the ring, resulting in the product.

The geometries of the critical points for Reactions 5–8 are analogous to those of Reactions 1–4. For that reason, we have not included drawings of them except for the intermediates. The pathways for Reactions 7 and 8 clearly contain intermediates. These intermediates have S–Se and S–S distances comparable to the intermediates of acyclic reactions (Figure 3). Inspection of the intermediate geometries reveals that they follow the same structural trend as noted for the intermediates of Reactions 3 and 4; namely, as the ring becomes bigger, the intermediate geometry approaches that of the intermediate of the acyclic

(28) Gonzales, J. M.; Cox, S. C. I.; Brown, S. T.; Allen, W. D.; Schaefer, H. F. I. *J. Phys. Chem. A* **2001**, *105*, 11327–11346.

(29) (a) Check, C. E.; Gilbert, T. M. *J. Org. Chem.* **2005**, *70*, 9828–9834. (b) Grimme, S. *Angew. Chem., Int. Ed.* **2006**, *45*, 4460–4464. (c) Schreiner, P. R.; Fokin, A. A.; Pascal, R. A.; deMeijere, A. *Org. Lett.* **2006**, *8*, 3635–3638. (d) Wodrich, M. D.; Corminboeuf, C.; Schleyer, P. v. R. *Org. Lett.* **2006**, *8*, 3631–3634.

(30) Perdew, J. P.; Burke, K.; Ernzerhof, M. *Phys. Rev. Lett.* **1996**, *77*, 3865–3868 (errata **1997**, *78*, 1396).

(31) (a) Zhao, Y.; Truhlar, D. G. *J. Chem. Theory Comput.* **2006**, *2*, 1009–1018. (b) Zhao, Y.; Truhlar, D. G. *J. Chem. Theory Comput.* **2007**, *3*, 289–300.

TABLE 4. Energies (kcal mol<sup>-1</sup>) Relative to Isolated Reactants for Reactions 5–8<sup>a</sup>

Reaction	IDC	TS1	INT	TS2	P	PTP
5S	-12.79	-12.78			-30.18	-27.45
5Se		-10.37			-34.82	-34.18
6S	-14.27	-9.22			-22.83	-24.79
6Se		-10.57			-29.94	-32.17
7S	-11.48	-8.57	-12.81	2.31	-3.03	-10.48
7Se		-10.10	-19.58	-0.14	-4.35	-15.93
8S(chair)	-10.66	-7.80	-10.76	4.24	2.25	-5.16
8Se(chair)		-10.14	-18.10	3.82	-1.78	-10.35
8S(boat) <sup>b</sup>	-6.92	-0.97	-7.87	2.46		
8Se(boat) <sup>b</sup>		-4.99	-13.64	-0.39		

<sup>a</sup> B3LYP/6-31+G(d) energies including ZPE. <sup>b</sup> Energies relative to the chair conformation of **8**. **8(boat)** are 4.57 kcal mol<sup>-1</sup> higher in energy than **8(chair)**.

analogue. Another interesting trend observed in the intermediates is the nearly equivalent sum of the bond distances to the hypercoordinate S or Se, about 5.18 Å.

The nature of the critical point that follows the first transition state for all reactions of the four-membered rings **2** and **6** requires further discussion. These critical points are all local minima and could be either intermediates or products. We favor the latter interpretation based on the following characteristics. First, the distances of the bonds to the heteroatom under attack are atypical of intermediates. The nucleophile–heteroatom distances are short, and the breaking heteroatom–heteroatom distances are very long. For example, the Se–S distance in **P-2S** is almost 0.3 Å shorter than that in the intermediate for the reaction of HS<sup>-</sup> with CH<sub>3</sub>SeSeCH<sub>3</sub>, and only 0.1 Å longer than a typical Se–S bond, suggesting that this bond is nearly fully formed. In **P-6S** and **P-6Se**, the breaking S–Se bond is more than 0.2 Å longer than that in the intermediates of Reactions 7 and 8. Second, these structures are much more energetically stable (by 10 kcal mol<sup>-1</sup>) than the intermediates. Their relative energies are more comparable to those of the products of the three-membered rings. The low energy of **P-2** and **P-6** suggests that the ring strain energy of the four-membered ring has been fully released, indicative of a product and not an intermediate where the ring is still extant. We drew a similar conclusion with the substitution reaction of 1,2-dithietane.<sup>11</sup>

The relative energies of the critical points on the potential energy surfaces for Reactions 5–8 are listed in Table 4. Both reactions of **5** and **6** follow the two-well surface, represented in Scheme 1. The reactions involving the larger cyclic selenenyl sulfides follow the three-well PES as represented in Scheme 2.

As with Reactions 1–4, all of the nucleophilic substitution reactions of selenenyl sulfides are exothermic, though Reaction 8S is only exothermic when one considers the proton-transfer product **PTP-8S**. The reactions become less exothermic with increasing ring size. This reflects relief of ring strain energy (vide infra).

The intermediates of Reactions 7 and 8 lie in a potential energy well characterized by the height of the entrance and exit barriers. For these reactions, the exit barrier is higher than the entrance barrier. In fact, the exit barrier is at or above the energy of the reactants. This behavior is identical that seen with the diselenides and disulfides.<sup>11</sup>

There are distinct energetic differences between attack at the sulfur or selenium of the selenenyl sulfides **5–8**. First, the overall reaction for attack at the selenium of all four rings is more exothermic than the attack at sulfur. This energetic preference ranges from 4.64 kcal mol<sup>-1</sup> in Reaction 5 to 1.32

TABLE 5. Ring Strain Energy (kcal mol<sup>-1</sup>) of 1–8<sup>a</sup>

	B3LYP	MP2		B3LYP		B3LYP
<b>1</b>	24.1	24.2	<b>5</b>	21.5	CH <sub>2</sub> S <sub>2</sub>	18.7
<b>2</b>	22.6	23.8	<b>6</b>	20.4	(CH <sub>2</sub> ) <sub>2</sub> S <sub>2</sub>	20.8
<b>3</b>	5.2	4.6	<b>7</b>	3.8	(CH <sub>2</sub> ) <sub>3</sub> S <sub>2</sub>	5.8
<b>4</b> (chair)	-0.4	-1.6	<b>8</b> (chair)	0.6	(CH <sub>2</sub> ) <sub>4</sub> S <sub>2</sub>	2.0
<b>4</b> (boat)	5.4		<b>8</b> (boat)	5.2	(CH <sub>2</sub> ) <sub>4</sub> S <sub>2</sub>	6.6
					(boat)	

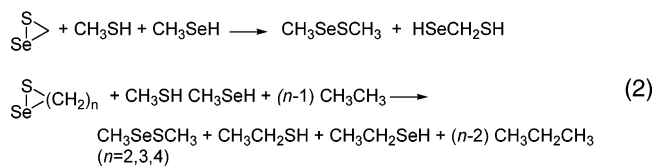
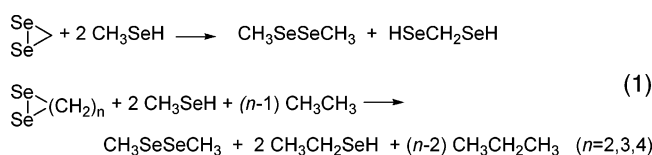
<sup>a</sup> Evaluated at B3LYP/6-31+G(d) using eq 1 or 2. Disulfide results from ref 11.

kcal mol<sup>-1</sup> in Reaction 7. The preference for attack at selenium is larger if one considers the proton-transfer products; in that case, selenium attack is favored by 5.5–7.5 kcal mol<sup>-1</sup>.

In all four reactions where intermediates are observed, the intermediate from attack at selenium is lower in energy than the intermediate from attack at sulfur. The energetic preference for the selenium intermediate is about 6–7 kcal mol<sup>-1</sup>.

Last, except for **TS1-5S** and **TS1-5Se**, the transition states for attack at selenium are lower in energy than those for attack at sulfur. In Reaction 5, the barrier for attack at sulfur is 2.4 kcal mol<sup>-1</sup> lower than for attack at selenium. For Reaction 6, **TS1-6Se** is 1.4 kcal mol<sup>-1</sup> below **TS1-6S**. For the other two reactions, we focus on the higher of the two transition states. With Reaction 7, the second transition state with attack at selenium is favored by 2.4 kcal mol<sup>-1</sup> over sulfur attack. Reaction 8 actually favors reaction through the boat conformation, and again the selenium pathway is favored over the sulfur path.

**Ring Strain Energy.** The ring strain energy (RSE) of 1–8 was evaluated using the group equivalent method.<sup>32</sup> The RSE is defined as the negative of either eq 1 or 2, and values are listed in Table 5. Experimental values are not available for comparison. However, the trends in strain energy for these cyclic compounds—RSE decreases with increasing ring size and the three-membered rings are slightly more strained than the four-membered rings—mimic strongly those we reported for cyclic disulfides,<sup>11</sup> whose values are reproduced in Table 5.



## Discussion

The mechanism of nucleophilic substitution at sulfur or selenium can be distinguished by the presence or absence of an intermediate. If the path has no intermediate, then the nucleophile adds as the leaving group exits, the S<sub>N</sub>2 mechanism. On the other hand, if an intermediate is traversed, then a two-step mechanism is invoked. First, the nucleophile adds to create the intermediate, and in a distinct second chemical step, the leaving group exits. This is an addition–elimination mechanism.

We have noted a broad range of substitution reactions at sulfur that follow the addition–elimination pathway.<sup>5–11</sup> Model reactions for nucleophilic substitution at selenium also indicate an A–E reaction.<sup>13</sup>

Our study on nucleophilic substitution at sulfur in cyclic disulfides revealed that ring strain energy can alter the mechanism.<sup>11</sup> Namely, substitution reactions of the strained three- and four-membered cyclic disulfides proceed via the S<sub>N</sub>2 reaction, while the larger and less strained five- and six-membered rings follow the A–E path.

Nucleophilic substitution reactions involving the selenium-containing cyclic compounds examined in this study (1–8) also show this mechanistic dependence on the ring size. The substitution reactions of the three-membered rings (1 and 5) all have potential energy surfaces that are topologically identical to that shown in Scheme 1. This surface is characterized by having no intermediate. A single transition state takes the IDC into the product. This S<sub>N</sub>2 mechanism is followed for the reaction of 1 regardless of nucleophile used and for reaction of 5 at either sulfur or selenium. Consistent with the S<sub>N</sub>2 mechanism, the incoming nucleophile attacks from the backside. Since these are very early transition states, the angle formed by the nucleophile, the heteroatom under attack, and the leaving group is much smaller than the paradigmatic value of 180°.

The S<sub>N</sub>2 mechanism operates for the substitution reactions of the four-membered rings 2 and 6. Here again, the reactions have no intermediates, though the products (**P-2S**, **P-2Se**, **P-6S**, and **P-6Se**) have some attributes that resemble the intermediates observed in other addition–elimination reactions involving substitution at sulfur and selenium. The distance between the heteroatoms that were bonded in the four-membered reactants is very long relative to that in true intermediates. Some interaction may still exist between these heteroatoms; these *gauche* product conformations are lower in energy than their *anti* isomers. Nonetheless, as argued in the Results section, an intermediate of the type seen in true addition–elimination reactions, like those involving the five- and six-membered rings, is not observed. Substitution reactions involving the larger five- and six-membered rings proceed via the addition–elimination mechanism, characterized by a stable intermediate on the reaction pathway.

Ring strain is the obvious culprit for these differences. The three- and four-membered cyclic diselenides, disulfides, and selenenyl sulfides are more strained than their five- and six-membered ring congeners. The strain energy in the small rings ranges from 18 to 24 kcal mol<sup>-1</sup>. The five-membered rings are substantially less strained, with RSEs of 4–6 kcal mol<sup>-1</sup>. The six-membered rings are essentially unstrained. Relief of ring strain is a strong driving force in the reactions of 1, 2, 5, and 6. This can be seen in the overall reaction energies, which are much more exothermic for the reactions of these small rings, ranging from –25 to –38 kcal mol<sup>-1</sup>, than for the five- and six-membered rings, whose reaction energies are exothermic by only a few kcal mol<sup>-1</sup> without considering the proton-transfer products.

One argument for the S<sub>N</sub>2 mechanism for reactions at small rings is that as the heteroatom–heteroatom bond begins to lengthen the ring strain is released, driving the full cleavage of the bond. This is an extension of the argument by Gronert and Lee that formation of small rings occurs through essentially

(32) Bachrach, S. M. *J. Chem. Educ.* **1990**, *67*, 907–908.

**TABLE 6.** Relative Energies (kcal mol<sup>-1</sup>) of Model Geometries of the Intermediate<sup>a</sup>

**A**

$\alpha$ (deg)	Se–Se–Se rel <i>E</i>	S–Se–S rel <i>E</i>	S–S–Se rel <i>E</i>	S–S–S <sup>b</sup> rel <i>E</i>
90	0.0	0.0	0.0	0.0
80	2.4	2.0	3.0	1.7
70	7.8	8.7	12.5	9.2
60	26.2	29.3	37.4	30.8

<sup>a</sup> The order of the heteroatoms is X<sub>1</sub>–X<sub>2</sub>–X<sub>3</sub>. Geometry optimized at B3LYP/6-31+G(d) with  $r(\text{X}_2\text{--X}_3)$  fixed as  $r(\text{Se--Se}) = 2.65 \text{ \AA}$  and  $r(\text{Se--S}) = r(\text{S--Se}) = r(\text{S--S}) = 2.5 \text{ \AA}$  and  $\alpha$  fixed to specific values. <sup>b</sup> Values from ref 11.

strain-free transition states.<sup>33</sup> For example, the reaction of HSCH<sub>2</sub>CH<sub>2</sub>S<sup>-</sup> to form thiirane has a barrier of 19.2 kcal mol<sup>-1</sup>, almost 6 kcal mol<sup>-1</sup> lower than the barrier for the reaction of ethylsulfide with MeS<sup>-</sup>. They argue that the strain energy of the four-membered ring is accrued *after* the transition state. In our case—the reverse of the ring formation examined by Gronert—the strain energy is released *before* the transition state is reached. The implication is that, for the strained rings, no intermediate can be achieved, and the mechanism is S<sub>N</sub>2.

A second argument is based on the ability of the heteroatom to accommodate an additional ligand, that is, to become hypercoordinate. To assess this, we expand on the model we described in the study of cyclic disulfides. A model intermediate **A** (see Table 6) is constructed such that the X<sub>2</sub>–X<sub>3</sub> distance is fixed to a value typical of acyclic intermediates (2.65 Å for Se–Se and 2.5 Å for all other combinations), and the C–X<sub>2</sub>–X<sub>3</sub> angle (called  $\alpha$ ) is held fixed. All other variables are allowed to optimize. Varying  $\alpha$  allows us to mimic the angles in a small ring environment and test the ability of a heteroatom to bind an additional ligand: the incoming nucleophile in our case. The relative energies for four values of  $\alpha$  are listed in Table 6. With all four heteroatom pairs, the energy rises appreciably only after the angle  $\alpha$  has been reduced to 70° and becomes quite large to 60°. These small values of  $\alpha$  are what would occur if there was an intermediate involving a three- or four-membered ring. Were a nucleophile to add to the heteroatom in these small rings, the strain energy would simply become too great, and instead of forming an intermediate, the ring breaks open. On the other hand, the value of  $\alpha$  in the intermediates formed from the five- and six-membered rings is always between 80 and 90°; for example, it is 83.3° in **INT-7Se**, 86.2° in **INT-7S**, 86.9° in **INT-4Se(chair)**, and 87.1° in **INT-4S(chair)**. The nucleophile can be readily accommodated in these larger rings, and so an intermediate is observed.

The mechanism for nucleophilic substitution at selenium (just as for sulfur) appears to be independent of the nature of the nucleophile. The reactions of **1** and **2** is S<sub>N</sub>2 and that of **3** and **4** is A–E, whether the nucleophile is HS<sup>-</sup> or HSe<sup>-</sup>. Furthermore, though B3LYP predicts larger differences in activation barriers and overall reaction energies than does MP2, both methods agree that barriers are lower and reactions are more exothermic with HSe<sup>-</sup> than with HS<sup>-</sup>. This thermodynamic preference is seen in the model Reactions 9 and 10 involving simple acyclic diselenides (Table 7). The intermediates involving

(33) (a) Gronert, S.; Lee, J. M. *J. Org. Chem.* **1995**, *60*, 4488–4497. (b) Gronert, S.; Lee, J. M. *J. Org. Chem.* **1995**, *60*, 6731–6736.

**TABLE 7.** Reaction Energies (kcal mol<sup>-1</sup>) for Model Acyclic Reactions<sup>a</sup>

		$\Delta E$ (B3LYP)	$\Delta E$ (MP2)
Reaction 9	CH <sub>3</sub> SeSeCH <sub>3</sub> + HS <sup>-</sup> → HSeSeCH <sub>3</sub> + CH <sub>3</sub> Se <sup>-</sup>	14.12	11.32
	CH <sub>3</sub> SeSeCH <sub>3</sub> + HSe <sup>-</sup> → HSeSeCH <sub>3</sub> + CH <sub>3</sub> Se <sup>-</sup>	10.10	10.21
Reaction 10	CH <sub>3</sub> SeSeCH <sub>2</sub> Se <sup>-</sup> + HS <sup>-</sup> → HSeSeCH <sub>2</sub> Se <sup>-</sup> + CH <sub>3</sub> Se <sup>-</sup>	10.30	9.50
	CH <sub>3</sub> SeSeCH <sub>2</sub> Se <sup>-</sup> + HSe <sup>-</sup> → HSeSeCH <sub>2</sub> Se <sup>-</sup> + CH <sub>3</sub> Se <sup>-</sup>	6.76	9.01

<sup>a</sup> Computed at B3LYP/6-31+G(d) or MP2/6-31+G(d) including ZPE.

attack with HSe<sup>-</sup> are also lower in energy than those involving attack by HS<sup>-</sup>. HSe<sup>-</sup>, being more polarizable than HS<sup>-</sup>, is the better nucleophile.

It is also worth commenting upon the similarities between substitution reactions of the diselenides and disulfide rings. The mechanism for substitution of the three- and four-membered ring disulfides and diselenides is S<sub>N</sub>2, while substitution occurs by the A–E mechanism with the five- and six-membered rings. The reaction of 1,2-dithiolane (the five-membered cyclic disulfide) is faster than that of 1,2-dithiane (the six-membered cyclic disulfide).<sup>34</sup> We found that (a) the intermediate for attack of 1,2-dithiolane is more stable than that of 1,2-dithiane; (b) the barrier for attack of the five-membered ring is higher than that of the six-membered ring; and (c) the reaction of 1,2-dithiolane is more exothermic than that of 1,2-dithiane. These same trends are exhibited by the diselenides: the reactions of **3** are both more exothermic and have a lower barrier than those of **4**, and the intermediates derived from **3** are more stable than the intermediates from **4**.

Our results reinforce the notion that nucleophilic substitution at sulfur and selenium preferentially proceeds by the addition–elimination mechanism. It is only with the perturbation of a small ring that the mechanism switches to the alternate S<sub>N</sub>2 mechanism. Evidence is now mounting that nucleophilic substitution at atoms other than first-row elements dominantly follow the addition–elimination pathway. Bickelhaupt's recent study<sup>35</sup> of nucleophilic substitution at phosphorus finds the addition–elimination pathway, confirming our earlier study.<sup>3</sup> Extensive studies of substitution at silicon also show the addition–elimination mechanism.<sup>36</sup> The S<sub>N</sub>2 mechanism operates at carbon and other first-row elements, where accommodation of an additional bond cannot happen, from either molecular orbital or steric points of view.

The other major issue addressed in this study is the potential selectivity of nucleophilic attack at selenium versus sulfur. Our initial study on this question examined simple acyclic selenenyl sulfides, where we found both a kinetic and thermodynamic preference for substitution at selenium.<sup>13</sup> Reactions 5–8 extend this study to the cyclic selenenyl sulfides. In all aspects, attack at selenium is preferred over attack at sulfur. These computational results are consistent with the recent experiments of Sarma and Mugesh.<sup>17</sup> They found essentially no substitution reactions at sulfur of selenenyl sulfides unless activating groups were present as in the drug ebselen.

(34) Singh, R.; Whitesides, G. M. *J. Am. Chem. Soc.* **1990**, *112*, 6304–6309.

(35) vanBochove, M. A.; Swart, M.; Bickelhaupt, F. M. *J. Am. Chem. Soc.* **2006**, *128*, 10738–10744.

(36) (a) Bento, A. P.; Solà, M.; Bickelhaupt, F. M. *J. Comput. Chem.* **2005**, *26*, 1497–1504. (b) Windus, T. L.; Gordon, M. S.; Davis, L. P.; Burggraf, L. W. *J. Am. Chem. Soc.* **1994**, *116*, 3568–3579. (c) Gronert, S.; Glaser, R.; Streitwieser, A. *J. Am. Chem. Soc.* **1989**, *111*, 3111–3117.



Kinetic preference is decidedly in favor of attack at selenium. For Reactions 5 and 6, which proceed via the  $S_N2$  mechanism, the transition state involving attack at selenium is lower than that of attack at sulfur: **TS1-5Se** lies 2.41 kcal mol<sup>-1</sup> below **TS1-5S** and **TS1-6Se** is 1.15 kcal mol<sup>-1</sup> below **TS1-6S**. For Reactions 7 and 8, the second transition state is rate-limiting. **TS2-7Se** is 2.45 kcal mol<sup>-1</sup> below **TS7-S**; in fact, this later TS lies above the energy of separated reactants. For the reaction of **8**, the only path through **TS2-8Se(boat)** avoids a transition state that is higher in energy than reactants. Even the first transition states are more favorable for attack at selenium than at sulfur.

Thermodynamic preference for attack at selenium is noted in two aspects. First, the overall reaction is more exothermic when the attack occurs at selenium than when it occurs at sulfur. Reaction 7 shows the least preference, where **P-7S** is only 1.32 kcal mol<sup>-1</sup> higher in energy than **P-7Se**. However, the preference for selenium is enhanced if one considers the proton-transfer product; the smallest preference is now 5.19 kcal mol<sup>-1</sup> in Reaction 8.

The intermediates of Reactions 7 and 8 created by attack at selenium are more stable than those formed by attack at sulfur. This energy difference is significant: **INT-7Se** is 6.77 kcal mol<sup>-1</sup> more stable than **INT-7S** and the difference in energy of **INT-8Se** and **INT-8S** is 7.34 kcal mol<sup>-1</sup>. These values are consistent with our study of nucleophilic substitution of acyclic diselenides (see Table 3). Selenium is better able to take on the additional ligand, accommodating a hypercoordinate environment, than is sulfur. This is due to selenium being larger than sulfur, so that it has room to fit a third species, and has energetically closer orbitals, which enhances its ability to participate in four-electron/three-center bonding.<sup>37</sup>

Extrapolating gas-phase results to the solution phase can be treacherous given that solvent can dramatically alter reaction rates especially for charged species. Nonetheless, the gas-phase results do mimic the limited experimental results for nucleophilic substitution of acyclic species; that is, substitution at selenium is faster than at sulfur. We are currently investigating the effect

of water on nucleophilic substitution reactions at selenium in cyclic and acyclic species and will report these results in due course.

## Conclusions

Gas-phase nucleophilic substitution reactions at selenium in acyclic diselenides occur by the addition–elimination reaction. We examined substitution at selenium in the parent three-, four-, five-, and six-membered cyclic diselenides. For the larger, less strained five- and six-membered rings, substitution again occurs via the addition–elimination route. However, relief of ring strain accompanies nucleophilic attack at the three- and four-membered diselenides, indicating a change of mechanism to  $S_N2$ . This behavior is identical to that of the cyclic disulfides. There is now substantial evidence that the standard pathway for gas-phase nucleophilic substitution at heteroatoms beyond the first row is the addition–elimination mechanism.

Selectivity for nucleophilic substitution at selenium over sulfur was demonstrated in cyclic selenenyl sulfides. The mechanism for this substitution was independent of which heteroatom is attacked; the size of the ring dictates the mechanism. The small, strained three- and four-membered cyclic selenenyl sulfides react via the  $S_N2$  pathway, while the larger five- and six-membered rings react by the addition–elimination mechanism. Attack at selenium is favored in terms of both kinetics and thermodynamics for the reaction of all four cyclic selenenyl sulfides, consistent with recent experimental<sup>17</sup> studies. This enhanced reactivity toward selenium over sulfur provides a tantalizing hint as to why nature has incorporated selenocysteine in a number of proteins. The S–Se bridge in proteins looks to be more reactive toward nucleophiles than the conventional disulfide bridge. We reiterate our suggestion for further examination of reactions at selenium in selenoproteins.

**Acknowledgment.** We thank the Robert A. Welch Foundation (W-1442), the National Science Foundation (CHE-0307260), and Trinity University for financial support of this research.

**Supporting Information Available:** Figures S1 and S2, the coordinates of all critical points for Reactions 1–4 at B3LYP/6-31+G(d) and MP2/6-31+G(d) and for Reactions 5–8 at B3LYP/6-31+G(d), their absolute energies, and number of imaginary frequencies. This material is available free of charge via the Internet at <http://pubs.acs.org>.

JO070578S

(37) (a) Hach, R. J.; Rundle, R. E. *J. Am. Chem. Soc.* **1951**, *73*, 4321–4324. (b) Pimentel, G. C. *J. Chem. Phys.* **1951**, *19*, 446–448. (c) Reed, A. E.; Schleyer, P. v. R. *J. Am. Chem. Soc.* **1990**, *112*, 1434–1445. (d) Kaupp, M.; van Wuelen, C.; Franke, R.; Schmitz, F.; Kutzelnigg, W. *J. Am. Chem. Soc.* **1996**, *118*, 11939–11950. (e) Landrum, G. A.; Goldberg, N.; Hoffmann, R. *J. Chem. Soc., Dalton Trans.* **1997**, 3605–3613.